Research Article

Modification of the Solid-State Nature of Sulfathiazole and Sulfathiazole Sodium by Spray Drying

Stefano Bianco,[1] Vincent Caron,[1] Lidia Tajber,[1] Owen I. Corrigan,[1] Lorraine Nolan,[1] Yun Hu,[2] and Anne Marie Healy[1,3]

Abstract. Solid-state characterisation of a drug following pharmaceutical processing and upon storage is fundamental to successful dosage form development. The aim of the study was to investigate the effects of using different solvents, feed concentrations and spray drier configuration on the solid-state nature of the highly polymorphic model drug, sulfathiazole (ST) and its sodium salt (STNa). The drugs were spray-dried from ethanol, acetone and mixtures of these organic solvents with water. Additionally, STNa was spray-dried from pure water. The physicochemical properties including the physical stability of the spray-dried powders were compared to the unprocessed materials. Spray drying of ST from either acetonic or ethanolic solutions with the spray drier operating in a closed cycle mode yielded crystalline powders. In contrast, the powders obtained from ethanolic solutions with the spray drier operating in an open cycle mode were amorphous. Amorphous ST crystallised to pure form I at ≤35 % relative humidity (RH) or to polymorphic mixtures at higher RH values. The usual crystal habit of form I is needle-like, but spherical particles of this polymorph were generated by spray drying. STNa solutions resulted in an amorphous material upon processing, regardless of the solvent and the spray drier configuration employed. Moisture induced crystallisation of amorphous STNa to a sesquihydrate, whilst crystallisation upon heating gave rise to a new anhydrous polymorph. This study indicated that control of processing and storage parameters can be exploited to produce drugs with a specific/desired solid-state nature.

KEY WORDS: amorphous state; dynamic vapour sorption; particle habit; physical stability; polymorphism; sulfathiazole.

INTRODUCTION

Depending on the conditions of evaporation, solidification from a solution may result in the generation of polymorphic or amorphous forms (1,2). These structural modifications are characterised by different energy states and therefore may undergo physicochemical transformations further on in the drug formulation manufacture pathway (3). These changes can also occur during storage as high-energy solid states tend, over time, to reach a lower energy level which is characterised by an increased physical stability (4). Examples of modification of a solid-state domain are the conversion of a compound into a different polymorphic or solvated structure, the transformation into its corresponding amorphous state (1) or, *vice versa*, crystallisation from the amorphous state. The solid-state nature of a compound determines its physicochemical and biopharmaceutical properties such as its solubility, dissolution rate, bioavailability and stability (3). It is generally desirable to produce a drug substance in its most stable form to avoid undesirable changes during processing or storage. However, the most stable form is not necessarily the one characterised by the best biopharmaceutical properties (5). A key aspect of innovation in drug product development is to produce a drug in its most useful solid-state form for the successful development of pharmaceutical preparations, even at the cost of reduced stability. Nevertheless, an adequate stability of a dosage form must be ensured and maintained within the limits imposed by pharmaceutical regulations (6).

Spray drying is a multifaceted process that may alter the solid-state nature of a drug (1,7,8). Several parameters must be taken into consideration in the spray drying process, such as feed concentration, spray dryer configuration, settings and solvent selection. The composition of the feed liquid in spray drying can have a significant effect on the properties of spray-dried products and can result in the production of powders with different degrees of crystallinity (9). Chidavaenzi *et al.* (9), for example, demonstrated that an increase in lactose content in the liquid feed resulted in a decrease of amorphous lactose in the spray-dried products.

Spray drying from non-aqueous systems on an industrial scale most commonly involves the closed-loop configuration. Nevertheless, there are numerous studies in the literature where laboratory-scale spray drying based on similar solvent systems were performed in the open-loop mode (1,7,10,11).

[1] School of Pharmacy and Pharmaceutical Sciences, University of Dublin, Trinity College, Dublin 2, Ireland.
[2] School of Chemistry, National University of Ireland, Galway, Ireland.
[3] To whom correspondence should be addressed. (e-mail: healyam@tcd.ie)

From this point of view, a comparison between the outcomes due to changes in the configuration is of interest, particularly in the context of scalability studies. Recently, Islam and Langrish (12) studied the effect of different spray drier configurations and drying and atomising gases (N_2, CO_2 and air) on the physicochemical properties of spray-dried lactose. Under different conditions, lactose in solution solidified into powders characterised by different properties. Despite similarities in the thermal properties, differences in the sorption behaviour were found and attributed to three reasons: a different degree of crystallinity, different surface morphology and particle size differences. Furthermore, the ability of a solvent to determine the final polymorphic form of a drug after crystallisation from solution has been shown, a process known as solution-mediated polymorphic transformations (13,14). The aim of the current work was to analyse the impact of spray drying parameters on the physical state of the model compound sulfathiazole, a sulphonamide drug known to present five different polymorphs (15,16), and on its corresponding sodium salt form.

The wide variety of physical states in which sulfathiazole can exist, including polymorphic, amorphous, salt and hydrate forms, make this compound an ideal subject for theoretical preformulation studies. The ability to understand, conceptualise and translate fundamental properties and behaviours from model compounds to current and newer systems has the potential to enhance our capabilities with the emergence of similar problematic active pharmaceutical ingredient (API).

MATERIALS AND METHODS

Materials

Sulfathiazole (ST) and sulfathiazole sodium (STNa) were purchased from Sigma (Ireland). Potassium bromide (KBr) was purchased from Spectrosol (Ireland) and stored in a desiccator over silica gel prior to the preparation of KBr discs. The solvents employed to prepare solutions for spray drying were acetone (analytical grade) and ethanol (99.5 %, *v*/*v*) from Corcoran Chemicals (Ireland) and deionised water produced by a Millipore Elix advantage water purification system.

Solubility Determination

Solubility in Water, Ethanol and Ethanol/Water Solvent Systems

The solubility of ST was determined in water, ethanol and ethanol/water mixtures (9:1, 8:2, 7:3, *v*/*v*). Excess solid was placed in 10-mL ampoules (Adelphi Tubes Ltd., UK) containing either 5 or 10 mL of the solvent and the ampoule was heat-sealed. The ampoules ($n=3$) were placed in a shaker water bath (100 cycles per minute, cpm) at 25 °C. After 24 h, each ampoule was opened and a sample withdrawn and filtered through a 0.45-µm membrane filter (Gelman Supor-450, USA). The concentration of the material was determined by a Shimadzu Pharmspec UV-1700 UV–Visible spectrophotometer ($\lambda=254$ nm) using 10-mm quartz cuvettes ($n=3$).

Solubility in Acetone and Acetone/Water Solvent Systems

The solubility of sulfathiazole was determined in acetone and three different acetone/water (*v*/*v*) ratios at 25 °C (9:1, 8:2, 7:3, *v*/*v*). Excess solid was placed in 12-mL ampoules ($n=3$, closed with screw caps to prevent evaporation) placed in a temperature-controlled (25 °C) water bath shaken at 100 cpm. The vials were kept under constant conditions up to 60 h and analysed at different time intervals (1, 6, 24, 48 and 60 h). The concentrations of filtrates from the acetonic systems were measured using a Shimadzu HPLC class VP series with a LC-10AT VP pump, SIL-10AD VP autosampler and SCL-10AVP system controller equipment operating with a SPD-10A VP UV–VIS spectrophotometer ($\lambda=254$ nm). A Hypersil BDS C18 5-µm column (length, 150 mm; Thermo Scientific) and a flow rate of 1 mL/min were employed using a method previously reported in the literature (17). The solubility of the drug in each solvent system was calculated as the average of the concentration values at the plateau of the corresponding concentration *versus* time curve ($n=3$).

Spray Drying

Spray-dried powders were obtained using a laboratory-scale Buchi B-290 Mini Spray Dryer (Buchi Laboratoriums-Technik AG, Flawil, Switzerland) operating either in an open cycle mode (OCM) configuration using air as the drying gas or in a closed cycle mode (CCM) configuration using nitrogen as the drying gas. ST feed systems (0.5 %, *w*/*v*) were prepared by dissolving the API in ethanolic or acetonic solvents, prepared by mixing ethanol or acetone with deionised water at different *v*/*v* ratios—9:1, 8:2 and 7:3. ST was also spray-dried as a solution from pure acetone and as a supersaturated solution from pure ethanol. Due to the higher solubility of the drug in acetonic solutions, ST was additionally dissolved in acetonic solutions in order to achieve a comparable degree of saturation to the ethanolic solutions. Spray drying of ST was performed using the following parameters: inlet temperature of 78 °C, gas flow of 40 mm (473 L/h), aspirator rate of 100 % and a feed flow rate of 30 % (8 mL/min). Additional details regarding feed concentrations, degree of saturation and outlet temperatures of the spray-dried systems are presented in Table I.

STNa solutions (0.5 %, *w*/*v*) were spray-dried from pure water, ethanol and ethanol/water solutions (9:1, 8:2, 7:3, *v*/*v*) in the OCM and from pure ethanol, ethanol/water and acetone/water solutions (9:1, 8:2, 7:3, *v*/*v*) in the CCM using spray drying parameters identical to those for ST, except for the inlet temperature which was set to 160 °C. The increase of the inlet temperature resulted in an outlet temperature ranging from 99 to 108 °C

Thermal Analysis

Differential scanning calorimetry (DSC) runs were conducted on a Mettler Toledo DSC 821^e using nitrogen as a purge gas. Samples (3–7 mg, $n \geq 2$) were placed in pin-holed aluminium pans and heated at a scanning rate of 10 °C/min from 25 to 220 °C for ST and from 25 to 280 °C for STNa. The thermograms were analysed with the Mettler Toledo STAR^e software.

Table I. Spray Drying Parameters for Sulfathiazole

Solvent	Spray dryer configuration	Volume ratio (v/v)	Outlet (°C) range	Feed concentration, % (w/v)	Degree saturation (%)
Ethanol	Open	1:0	52–56	0.5	120
Ethanol/water	Open	9:1	49–55	0.5	50
Ethanol/water	Open	8:2	48–52	0.5	35
Ethanol/water	Open	7:3	45–50	0.5	30
Ethanol/water	Closed	9:1	51	0.5	50
Ethanol/water	Closed	7:3	48–49	0.5	30
Acetone	Closed	1:0	58–59	0.5	42
Acetone/water	Closed	9:1	49–54	0.5	8
Acetone/water	Closed	8:2	48–50	0.5	7
Acetone/water	Closed	7:3	47–50	0.5	8
Acetone	Closed	1:0	57–58	1.2	100
Acetone/water	Closed	9:1	54–55	3	50
Acetone/water	Closed	8:2	49–50	2.45	35
Acetone/water	Closed	7:3	50–51	1.95	30

Modulated differential scanning calorimetry (MDSC) scans were recorded on a QA-200 TA instruments MDSC calorimeter using nitrogen as a purge gas. Weighed samples (1.5–3.5 mg, $n \geq 2$) were sealed in closed aluminium pans with one pinhole. The method selected was similar to that previously reported by Caron *et al.* (7). A scanning rate of 1 °C/min, amplitude of modulation of 1 °C and modulation frequency of 1/60 Hz were employed for all the experiments. The temperature range was from 5 to 200 °C.

Thermogravimetric Analysis

Thermogravimetric analysis (TGA) experiments were conducted on a Mettler Toledo TG 50 apparatus using a method previously described by (1). Weighed samples (5–10 mg, $n \geq 2$) were analysed in open aluminium pans placed on a Mettler MT5 balance. Samples were heated from 25 to 220 °C for ST and from 25 to 280 °C for STNa at a scanning rate of 10 °C/min under nitrogen purge. Mass loss of the samples recorded were analysed by the Mettler Toledo STARe software.

Powder X-Ray Diffraction

X-ray powder diffraction measurements were conducted on samples mounted on a low-background silicon sample holder using a Rigaku Miniflex II, desktop X-ray diffractometer (Japan). The method employed was as previously described (7). The samples were scanned over a range of 5–40° in 2θ scale using a step size of 0.05°/s. The X-ray source was a Cu Kα radiation ($\lambda = 1.542$ Å), and the diffractometer was operated with a voltage of 30 kV and a current of 15 mA.

Fourier Transform Infrared Spectroscopy

Infrared spectra were produced using a Nicolet Magna IR 560 E.S.P. spectrophotometer controlled by the OMNIC 4.1 software. The method used was as previously described (7). An average of 64 scans with a resolution of 2 cm^{-1} over a wavenumber region of 4,000–650 cm^{-1} was used for each sample. Powder samples were diluted with KBr in a ratio 1:100 (w/w) and then pressed under 8 tons for 2 min.

Scanning Electron Microscopy

SEM micrographs were recorded on a Mira Tescan XMU microscope (resolution, 3 nm at 30 kV; accelerating voltage, 5 kV; specimen stage, 300×330 mm (Compucentric); detector, secondary electron). Before analysis, the samples were fixed on aluminium stubs and coated with gold under vacuum. Different areas of each sample were analysed and photomicrographs were taken at different magnifications.

Dynamic Vapour Sorption

Unprocessed and spray-dried materials were analysed with a dynamic vapour sorption apparatus (DVS; Surface Measurement Systems, UK) using a method previously described (18). The samples ($n \geq 2$) placed in a microbalance located inside a temperature- (25 °C) and relative humidity-controlled cabinet were exposed to 10 % step changes in relative humidity from 0 to 90 % and back to 0 %. Each sample was submitted to three sorption–desorption cycles. Additionally, the sorption–desorption behaviour in the first sorption–desorption cycle was measured at RH values of 3 and 6 %. The apparatus was set up to allow the sample mass to reach equilibrium at each step ($dm/dt \leq 0.002$ mg/min for 10 min). Isotherms of sorption and desorption were then calculated. The amount of water adsorbed and/or absorbed was expressed as a percentage of the dry sample. The DVS apparatus was also employed to perform accelerated stability studies on ST. For these studies, different samples of the processed drug were exposed to different %RH values (50, 60, 65 and 70 %) for 1200 min.

Influence of Environmental Conditions (Temperature and Relative Humidity)

The physical stability of the amorphous form of ST and STNa was investigated as a function of humidity and temperature using an Amebis stability testing system (Ireland). Different samples were placed in Amebis humidity devices at <5, 35, 55 or 60 % RH and stored in Gallenkamp incubators at 25 or 40 °C.

RESULTS

Sulfathiazole

Solubility

The determined solubilities of unprocessed ST in ethanol, acetone, water, ethanol/water and acetone/water mixtures at different ratios (9:1, 8:2, 7:3, *v/v*) are listed in Table II. ST solubility in acetone was approximately three times higher than in ethanol. In contrast, the solubility in water was close to zero. By adding water to the ethanol and to the acetone, the properties of the solvents were modified. The solubility of the drug in the co-solvent mixtures increased up to three and six times the solubility in pure ethanol and acetone, respectively. The addition of an organic co-solvent to water makes the solvating environment less polar, resulting in a more favourable solvation of the hydrophobic ST in the liquid phase.

PXRD Analysis

Open Cycle Mode. The powder X-ray diffraction (PXRD) pattern of unprocessed ST (k in Fig. 1) was characterised by sharp Bragg peaks indicative of a crystalline structure, and it was found to be of form III (7). ST spray-dried from pure ethanol was partially crystalline, and by comparing the peak positions to theoretical patterns, low-intensity Bragg peaks of form I were detectable on the PXRD pattern, as indicated by the arrows in d in Fig. 1. In contrast, ST powders spray-dried from ethanol/water solutions at all compositions were amorphous with no diffraction peaks, but a characteristic halo pattern in the diffractograms of the materials (e in Fig. 1). PXRD analysis on the processed materials was carried out immediately after the end of the spray drying process (*t*=0). Spray-dried powders stored at ambient conditions (18–22 °C and 45–80 % RH) were subsequently analysed at different timescales following the end of the process: 30 min (*t*=1/2 h), 1 h (*t*=1 h) and ~24 h (*t*=24 h). The detection of Bragg peaks in the patterns of the materials spray-dried from ethanolic solutions at all compositions was possible after 30 min from the end of the process (f in Fig. 1). Samples stored at ambient conditions up to 1 h after processing presented Bragg peaks exclusively of form I (g in Fig. 1), a metastable polymorph of ST at room temperature, whilst the same samples analysed after 24 h were found to be a mixture of polymorphic forms.

Table II. Solubility Data for Sulfathiazole

API	Solvent	Volume proportions (*v/v*)	Concentration (mg/mL)
Sulfathiazole	Ethanol	1:0	4.13±0.15
Sulfathiazole	Ethanol/water	9:1	9.78±0.28
Sulfathiazole	Ethanol/water	8:2	14.65±0.50
Sulfathiazole	Ethanol/water	7:3	15.90±0.62
Sulfathiazole	Water	1:0	0.26±0.02
Sulfathiazole	Acetone	1:0	12.29±0.88
Sulfathiazole	Acetone/water	9:1	60.38±0.74
Sulfathiazole	Acetone/water	8:2	71.90±1.32
Sulfathiazole	Acetone/water	7:3	64.59±2.16

Extra diffraction peaks characteristic of form II and/or form III (15.2°, 15.5°, 20.0°, 21.6°, scattering angle 2θ) were visible together with those of form I (h in Fig. 1). Crystallisation occurred in a time span ranging from 1 to 24 h. The influence of temperature and RH on the crystallisation of amorphous ST was investigated by characterising the samples after storage at various controlled temperatures and RH. Regardless of the spray drying parameters, the PXRD patterns of spray-dried ST following storage at 40 and 25 °C and four different percentages of RH (5, 35, 55 and 60 %) showed that amorphous ST converted to form I when the storage temperature was either at 25 or 40 °C and the RH was kept at or below 35 % (i in Fig. 1). Peaks belonging to form II and/or III were detectable when the RH was increased to or above 55 %. This demonstrated that the type of recrystallising polymorph was dependent on the temperature and humidity of storage rather than on the solvent composition of the feed solution.
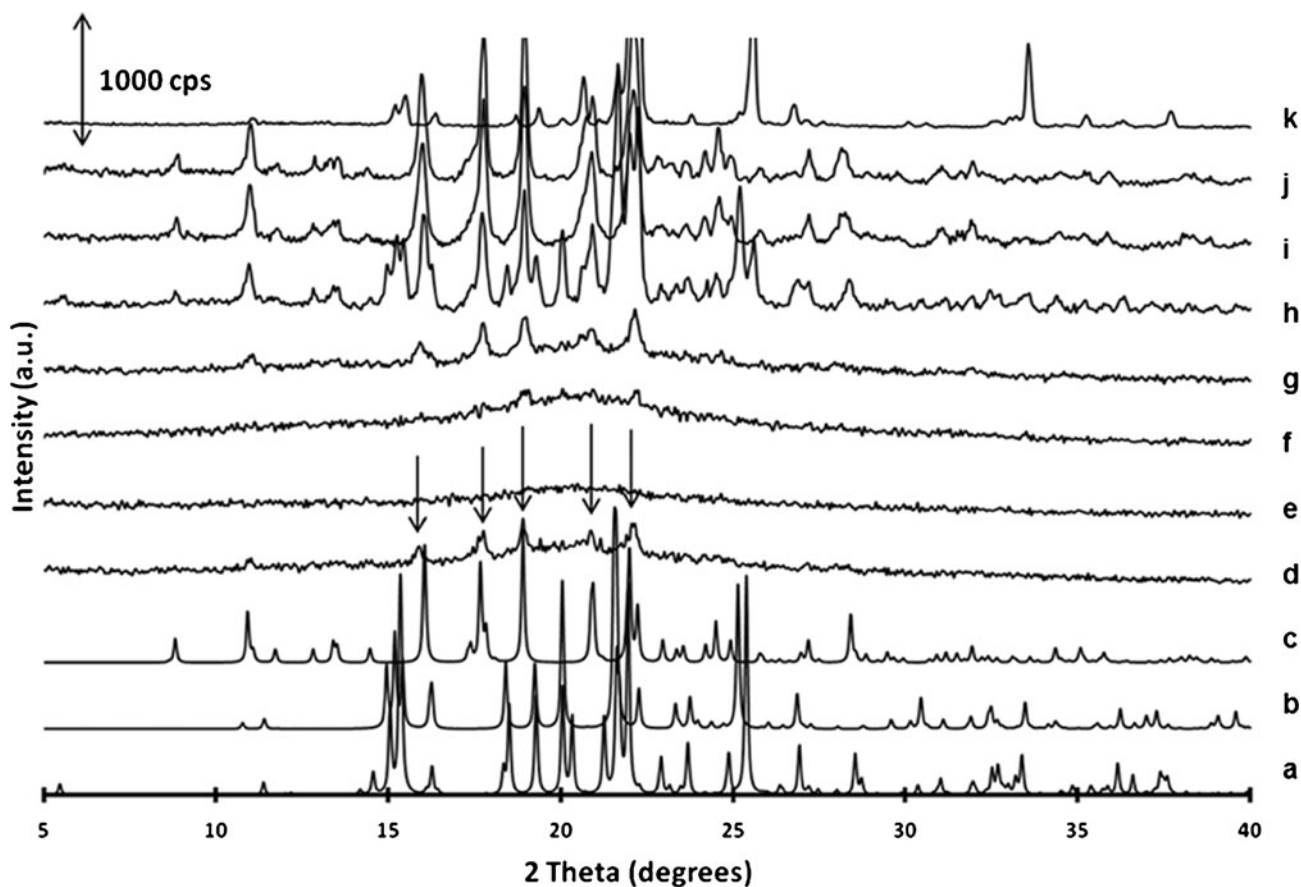
Closed Cycle Mode. Upon processing ST from both ethanolic and acetonic solutions, including pure ethanol and pure acetone, in a CCM configuration, the resulting powders subjected to XRD analysis immediately after the process (*t*=0) presented diffractograms characteristic of a crystalline material regardless of the organic solvent to water proportions or the feed concentration. ST powders processed in the CCM configuration from all solvent(s) systems presented PXRD patterns characteristic of form I (j in Fig. 1).

Thermal Analysis

Open Cycle Mode. The DSC thermogram of unprocessed ST was characterised by two endothermic events with onsets at 167±0.5 and 201±0.5 °C, respectively (f in Fig. 2). The first endotherm was attributed to a solid-state phase transition of form III into form I. The event with the higher temperature onset was consistent with the melting of ST form I (19). Thermal analysis confirmed PXRD results that ST before being processed was form III. In contrast, the DSC thermograms of spray-dried ST at *t*=0 from ethanolic solutions at all compositions including pure ethanol showed an exotherm with onset at 79±0.5 °C attributed to the crystallisation of the amorphous material and a melting event at 200±0.5 °C, characteristic of melting of form I (e in Fig. 2). The absence of thermal events between the endset temperature of the crystallisation peak and melting point indicated that thermal stress leads to the conversion of the amorphous material into pure form I, the polymorph which is stable at high temperatures. A completely PXRD amorphous sample was characterised by a ΔH equal to 38.80±0.75 J/g. The glass transition temperature, T_g, was detected at 59±0.8 °C by MDSC. DSC analysis was carried out simultaneously to PXRD analysis 30 min and 1 and 24 h after the end of the spray drying process for samples stored at ambient temperature and humidity. Crystallisation upon storage of ST powders, which was shown by the increase in intensity and number of Bragg peaks in PXRD patterns, was confirmed by the decrease of enthalpy of crystallisation in the thermograms of the spray-dried powders. The DSC thermograms of all spray-dried ST samples stored at ambient temperature and humidity for 24 h presented two endothermic events (d in Fig. 2). The enthalpy (ΔH) and onset temperature of the first event, attributed to the phase transition of form II

Fig. 1. PXRD patterns of ST form III (CCDC normalised theoretical PXRD pattern) **a**; ST form II (CCDC normalised theoretical PXRD pattern) **b**; ST form I (CCDC normalised theoretical PXRD pattern) **c**; spray-dried ST in OCM from ethanol (t=0) **d**; spray-dried ST in OCM from ethanol/water 9:1, v/v (t=0) **e**; spray-dried ST in OCM from ethanol/water 9:1, v/v (t=1/2 h) **f**; spray-dried ST in OCM from ethanol/water 9:1, v/v (t=1 h) **g**; spray-dried ST in OCM from ethanol/water 9:1, v/v (t=24 h) **h**; spray-dried ST in OCM from ethanol/water 9:1 (v/v) stored at 40 °C and <5 % RH **i**; spray-dried ST in CCM from acetone/water 9:1, v/v **j**; unprocessed ST (intensity divided by 3) **k**

and/or form III to form I, were not constant for different samples, indicating a variable amount of polymorphs in the completely crystallised products even for samples processed under the same spray drying conditions. Therefore, the influence of temperature and RH on the crystallisation of the samples spray-dried from the different ethanol/water ratios was studied by subjecting the samples to DSC analysis after storage for 24 h in different controlled conditions. Following storage at 25 and 40 °C, DSC analysis carried out on spray-dried ST confirmed that amorphous ST converted to pure form I when the RH was kept at or below 35 %. A single endothermic event attributed to melting at ~200 °C characterised the thermograms of the samples stored under these environmental conditions (b in Fig. 2). In contrast, the phase transition of form II and/or form III to form I was detectable when the storage RH was increased to 55 or 60 %. Under storage at <5 % RH, some residual amorphous material was still present within the material after 24 h (c in Fig. 2). Full crystallisation at <5 % RH occurred in a time span ranging from 24 to 72 h from the end of the process.

Closed Cycle Mode. DSC thermograms of ST spray-dried in the CCM from all solvent systems were distinguished by a

single endothermic event with onset at 197±0.5 and 199±0.5 °C for acetonic (a in Fig. 2) and ethanolic solutions respectively, attributable to the melting of form I. The increase in feed concentration for the acetonic systems did not affect the solid-state nature of the API.

SEM Analysis

Open Cycle Mode. Figure 3a, c shows the SE micrographs for spray-dried ST samples stored at 40 °C and <5 % RH and at ambient conditions, respectively. As can be observed in Fig. 3a, spray-dried ST samples after crystallisation into form I showed spherical particles with rough surfaces. In contrast, smooth platelets together with spherical particles could be observed when spray-dried ST crystallised into a mixture of polymorphs I and II/III (Fig. 3c). These platelets are consistent with the morphology of both form III, characteristic of the starting material (Fig. 3d), and of form II (20).

Closed Cycle Mode. Figure 3b shows the SE micrographs for ST samples spray-dried in the CCM from acetone/water. The particles ranged from spherical to irregularly shaped with rough surfaces.
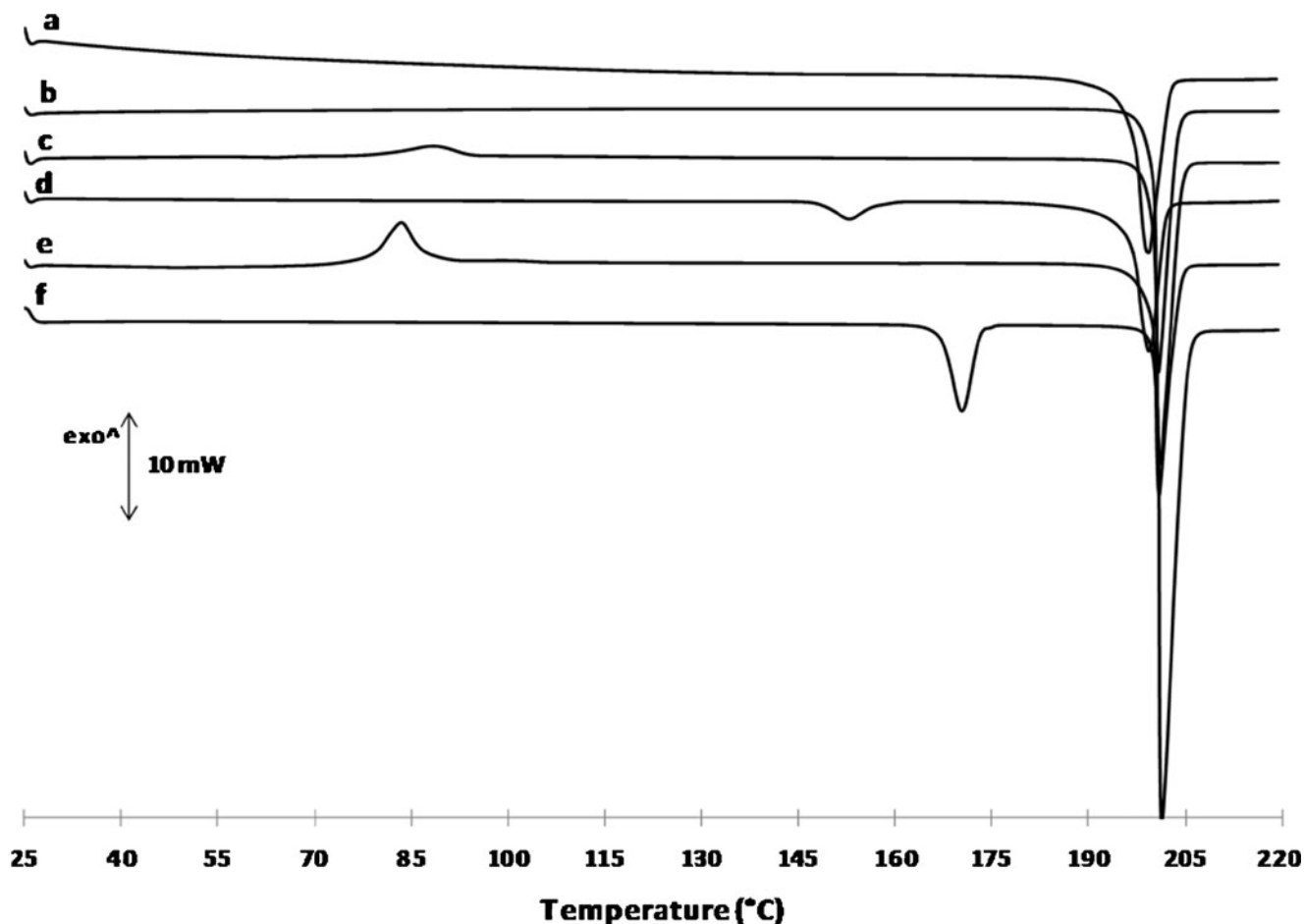
Fig. 2. DSC thermograms of spray-dried ST in CCM from acetone/water 9:1, *v/v* **a**; spray-dried ST in OCM from ethanol/water 9:1 (*v/v*) stored at 40 °C and <5 % RH after 72 h **b**; spray-dried ST in OCM from ethanol/water 9:1 (*v/v*) stored at 40 °C and <5 % RH after 24 h **c**; spray-dried ST in OCM from ethanol/water 9:1, *v/v* (*t*=24 h) **d**; spray-dried ST in OCM from ethanol/water 9:1, *v/v* (*t*=0) **e**; and unprocessed ST (form III) **f**

DVS Analysis

Sorption–desorption isotherms showed that unprocessed crystalline ST (form III), when exposed to a series of 10 % step changes of RH (0–90–0 %), reached a maximum water uptake of ~0.1 % at 90 % RH (a in Fig. 4). Form I was found to be more hygroscopic than the unprocessed material, with a maximum mass uptake of 0.54 % at 90 % RH (b in Fig. 4). No polymorphic change could be detected by PXRD after subjecting the powder to three full sorption–desorption cycles. In contrast, ST form I (b in Fig. 4) converted to a mixture of forms I and II and/or form III at the end of the three sorption–desorption cycle experiments. DSC and PXRD analyses showed the presence of the new form together with form I after subjecting ST form I samples to the critical RH of 65 %. In contrast, no phase transition was detected when the same experiment was carried out at RH values fixed at or below 60 %.

**Sulfathiazole Sodium**

PXRD Analysis

Open Cycle Mode. Unprocessed STNa presented a PXRD pattern typical of a crystalline substance (a in Fig. 5),

whilst the diffractograms of all the processed material patterns regardless of the solvent composition and ratio employed in the process appeared as amorphous halos (b–c in Fig. 5). For all amorphous salt powders, crystallisation of the materials was not observed over 12 months when stored in a dessicator at 4 °C.

Closed Cycle Mode. The powders collected after spray drying from acetone/water 9:1, *v/v* (d in Fig. 5) and from ethanolic solutions at all compositions presented an amorphous PXRD pattern and were immediately placed in controlled humidity devices at <5 % RH due to their physical instability. Under this storage RH, the powders did not recrystallise over 12 months. Concerning the other acetonic systems spray-dried in the CCM (water content in the feed above 10 %, *v/v*), the spray-dried powders converted in a few minutes to a sticky mass during sample collection and therefore were not analysed.

Thermal Analysis

Open Cycle Mode. The DSC scan of unprocessed STNa and the DSC and TGA thermograms of the material spray-dried from different solvents are shown in Fig. 6a. Unprocessed STNa presented an endothermic event attributable to the melting point at 268±0.2 °C. It was preceded by a small
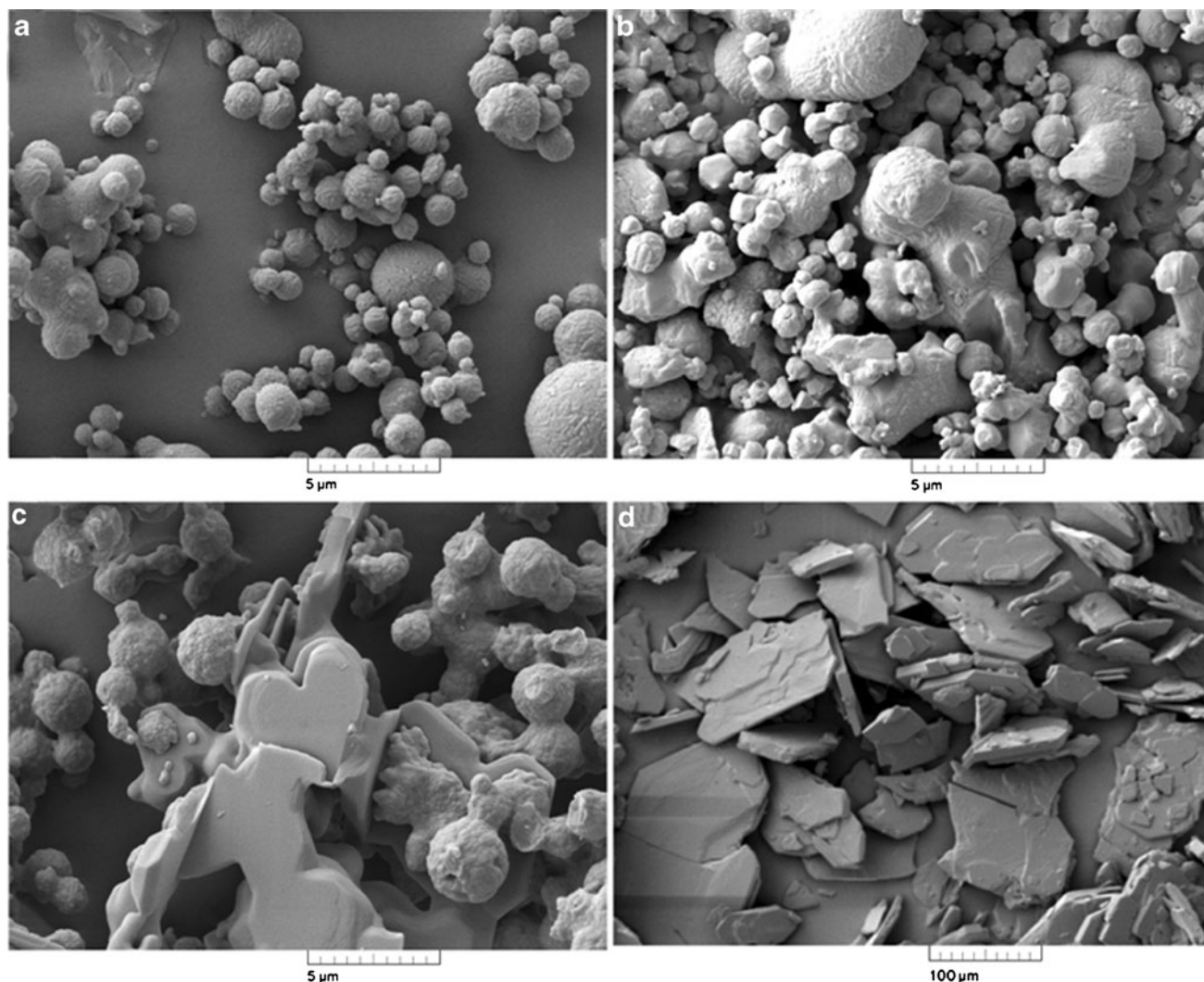
Fig. 3. SEM micrographs of spray-dried ST in OCM from ethanol/water 9:1 (*v/v*) stored at 40 °C and <5 % RH (form I) **a**; spray-dried ST in CCM from acetone/water 9:1, *v/v* (form I) **b**; spray-dried ST in OCM from ethanol/water 9:1 (*v/v*) stored at ambient conditions (forms I and III) **c**: and unprocessed ST (form III) **d**

endotherm appearing between 70 and 100 °C, attributed to solvent removal. TGA presented a mass loss of ~0.4 % between 25 and 100 °C and indicated that melting was accompanied by
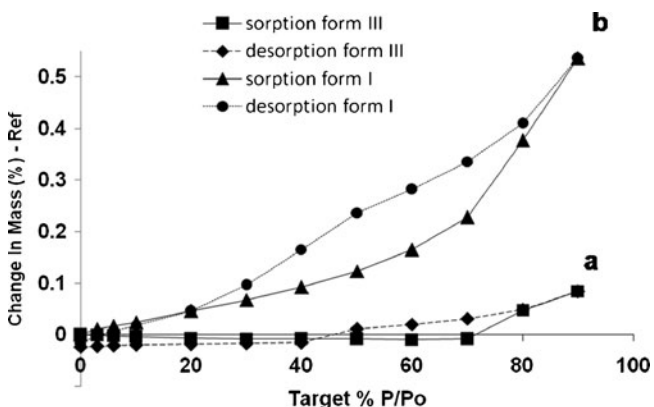
Fig. 4. Sorption–desorption isotherms of unprocessed ST (form III) **a** and spray-dried ST in OCM from ethanol water 9:1 (*v/v*) stored at 40 °C and 5%RH (form I) **b**

decomposition. The DSC thermograms of the processed powders presented an exotherm of crystallisation in the temperature range between 150 and 180 °C (Fig. 6a). The onset temperature of the exotherm was variable depending on the solvent composition of the feed solutions employed in the process. Higher onset temperatures were recorded when the materials were spray-dried from pure water, pure ethanol and ethanolic solutions with a water content at or below 20 % (*v/v*) compared to the systems spray-dried from ethanol/water 7/3 (*v/v*). A second exothermic peak, albeit of lower intensity, was observed above 175 °C on the thermograms of all the materials spray-dried in the OCM (Fig. 6a). The DSC thermograms were also characterised by a broad endotherm between 25 and 100 °C, attributable to weakly bonded or adsorbed solvent. A deflection of the baseline at ~120 °C was observed and attributed to the glass transition (T_g). Spray-dried STNa from ethanol and water 9:1 (*v/v*) was subjected to modulated calorimetry, and the reversing heat flow thermogram showed a deflection of the baseline at 122 °C, confirming the detection of T_g. The corresponding TGA thermograms of the spray-dried samples showed mass loss ranging from ~4.2 to 6.5 % between 25 and 130 °C. The solid-state
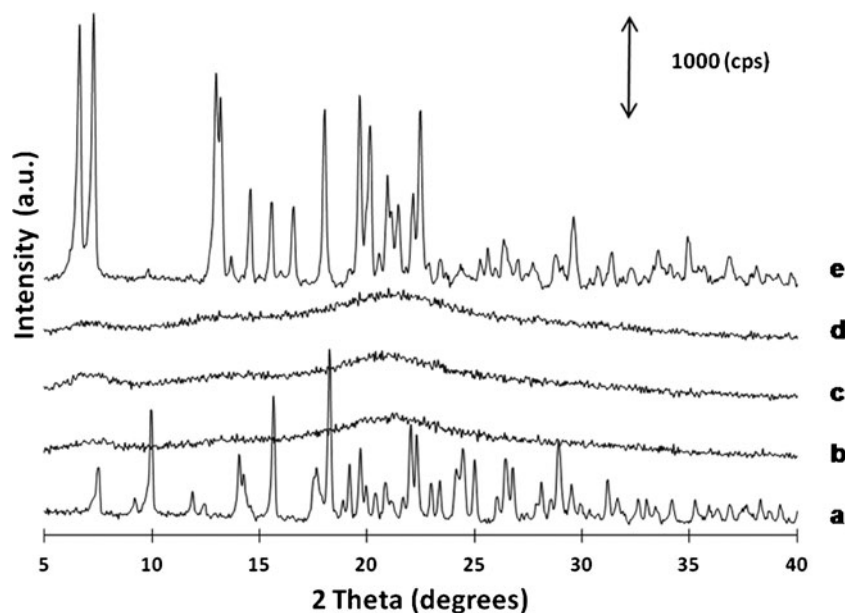
Fig. 5. PXRD patterns of unprocessed STNA **a**; spray-dried STNA in OCM from ethanol/
water 9:1, *v/v* **b**; spray-dried STNA in OCM from water **c**; spray-dried STNA in CCM from
acetone/water 9:1, *v/v* **d**; and unprocessed STNA after DVS **e**

changes of the processed drug during heating were studied
combining both DSC and PXRD techniques. The PXRD pat-
terns of STNa spray-dried from water, ethanol and ethanol/
water solutions (c, d, k in Fig. 7) heated up to 180 °C, above
the endset of the first exotherm peak, at a heating rate of 10 °C
per minute were all similar and differed from the pattern of the
crystalline unprocessed material (a in Fig. 7) by the presence of
extra peaks at the following 2θ values: 6.57°, 8.13°, 10.61°,
13.39°, 16.36°, 17.15°. The PXRD pattern of the materials heat-
ed at the same rate above the endset of the second exothermic
peak (~200 °C) was the same as the diffraction pattern of the
unprocessed material.

Closed Cycle Mode. The DSC thermograms of STNa
samples spray-dried from acetone/water showed tailing of
the exothermic peak (two peaks fused together) with onset
at ~150 °C (b in Fig. 6). The material presented two melting
peaks. The first peak was reported at 255 °C. The second peak
was recorded in the melting range of the powders obtained
from pure water and ethanolic systems at ~262 °C. A ~4.7 %
mass loss was determined by TGA between 25 and 130 °C. An
additional mass loss of about 1.1 % in the acetonic system was
detected in the same temperature range where the
corresponding DSC exotherm was recorded. When sub-
jected to modulated calorimetry, the reversing heat flow
thermogram for STNa from acetone and water 9:1 (*v/v*)
showed a deflection of the baseline in two steps at ~113 °C.
The thermal behaviour of STNa spray-dried from ethanolic
solution was dependent on the solvent ratio employed to
produce the feed solution. The systems spray-dried from
pure ethanol and ethanol/water 9:1 (*v/v*) were characterised
by a single exothermic peak (Fig. 6b). These crystallisation
peaks were recorded at the lowest temperatures for all
spray-dried systems either in the OCM or CCM. The
corresponding TGA thermograms were characterised by
mass loss in two steps: between 25 and 90 °C and between
95 and 150 °C. In contrast, the systems spray-dried from

ethanol/water with ethanol content at or below 80 %
(*v/v*) were characterised by two exothermic peaks, as pre-
viously seen for the systems spray-dried in the OCM, and
the corresponding TGA thermograms presented mass loss
in a single step (Fig. 6b). The PXRD patterns of the
material spray-dried from acetone/water 9:1 (*v/v*) heated
up to different temperatures—155, 175 and 230 °C—at a
heating rate of 10 °C/min differed from the pattern of the
crystalline unprocessed material (Fig. 7). New Bragg peaks
together with those of the unprocessed material were evi-
dent in the pattern of the material heated up to a temperature of
230 °C, above which no thermal events were observed apart
from melting.

DVS Analysis

In Fig. 8a–c, DVS isotherms of sorption–desorption (two
full cycles) of the original material and of the spray-dried
material obtained from ethanol/water 9:1 (*v/v*) in the OCM
and acetone/water 9:1 (*v/v*) in the CCM are shown. The iso-
therms showed that unprocessed STNa, when exposed to a
series of 10 % step changes of RH from 0 to 90 % and back to
0 %, was characterised by water uptake. The mass gain per-
centage was equal to 9.5±0.1 % (Fig. 8a). In contrast, STNa
spray-dried in the OCM from ethanol/water 9:1 (*v/v*) at the
end of the same experiment was characterised by a mass gain
of ~7.7 % (Fig. 8b). A lower mass gain by the end of the
analysis, of ~5.7 %, characterised the salt spray-dried in the
CCM from acetone/water 9:1, *v/v* (Fig. 8c). In the first sorption
cycle, no mass loss was detected from the ethanolic system at
any stage (Fig. 8b). In contrast, the acetonic system showed a
~2.7 % mass loss in the 40–50 % RH step, as indicated by the
arrow in Fig. 8c. All the materials analysed after DVS pre-
sented an identical PXRD pattern which differed from the
original material pattern (e in Fig. 5). A 9.8±0.4 % thermog-
ravimetric mass loss between 30 and 120 °C confirmed the
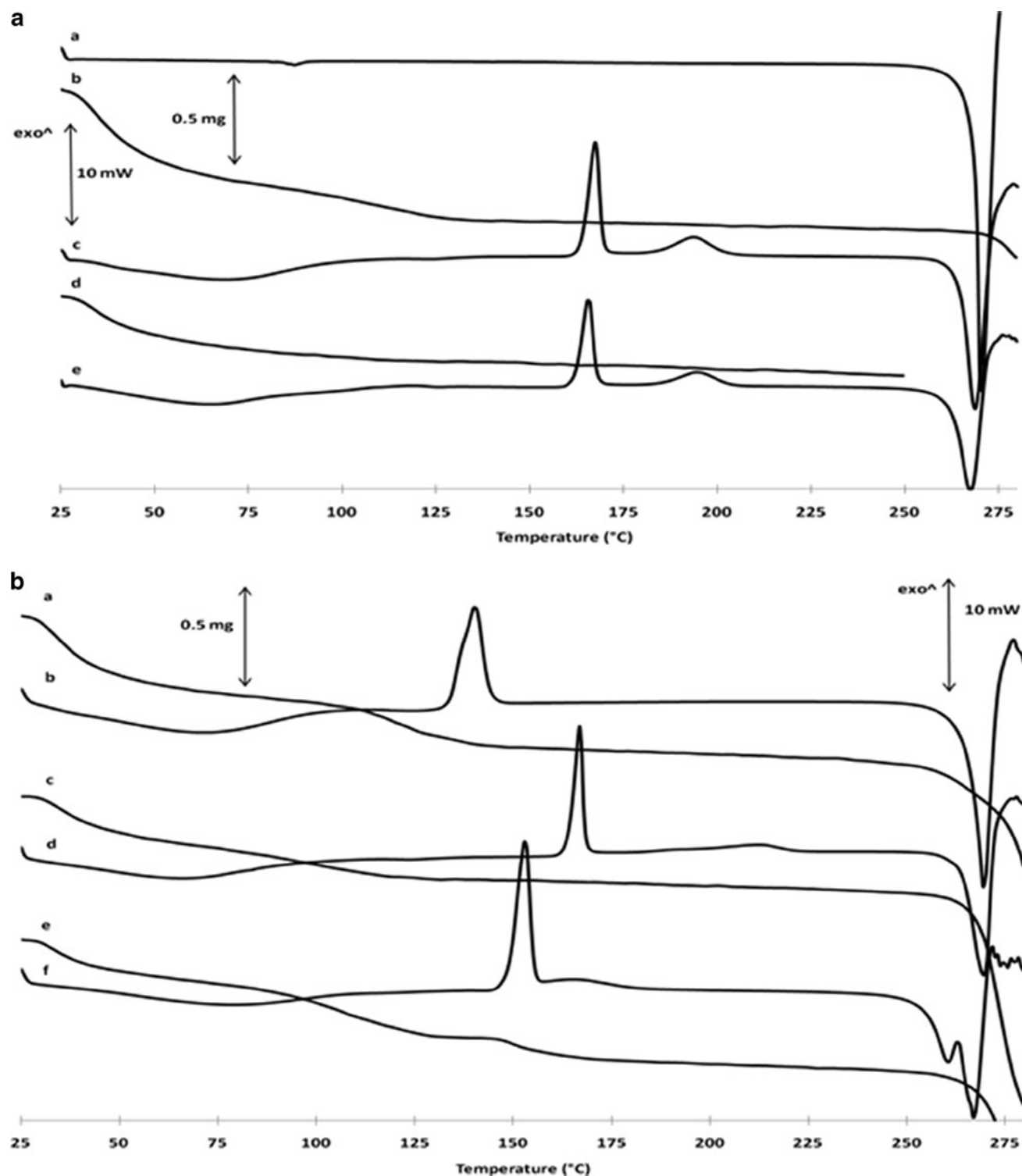
Fig. 6. a DSC analysis of unprocessed STNA **a**; TGA of spray-dried STNA in OCM from ethanol/water 9:1, *v/v* **b**; DSC analysis of spray-dried STNA in OCM from ethanol/water 9:1, *v/v* **c**; TGA of spray-dried STNA in OCM from water **d**; and DSC analysis of spray-dried STNA in OCM from water **e**. **b** TGA of spray-dried STNA in CCM from ethanol/water 9:1, *v/v* **a**; DSC analysis of spray-dried STNA in CCM from ethanol/water 9:1, *v/v* **b**; TGA of spray-dried STNA in CCM from ethanol/water 7:3, *v/v* **c**; DSC analysis of spray-dried STNA in CCM from ethanol/water 7:3 *v/v* **d**; TGA of spray-dried STNA in CCM from acetone/water 9:1, *v/v* **e**; DSC analysis of spray-dried STNA in CCM from acetone/water 9:1, *v/v* **f**

stoichiometry of the spray-dried material after DVS treatment to be a sesquihydrate (Fig. 9). The corresponding DSC thermogram showed a sharp endotherm in the same temperature range; the material consequently reconverted into its anhydrous form and finally melted at 268 °C, consistent with the melting point of unprocessed STNa.
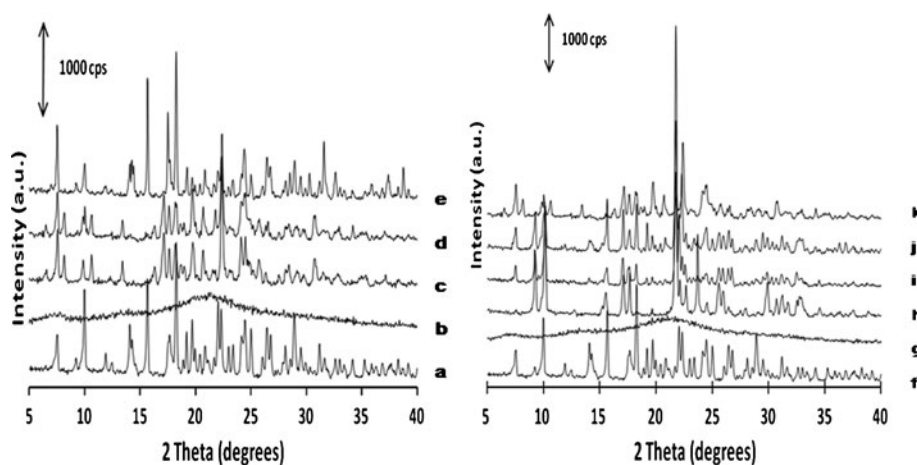
Fig. 7. XRD patterns of unprocessed STNA **a**; spray-dried STNA in OCM from ethanol/water 9:1, *v*/*v* **b**; spray-dried STNA in OCM from water, heated up to 180 °C **c**; spray-dried STNA in OCM from ethanol/water 9:1 (*v*/*v*), heated up to 180 °C **d**; spray-dried STNA in OCM from ethanol/water 9:1 (*v*/*v*), heated up to 210 °C **e**; unprocessed STNA **f**; spray-dried STNA in CCM from acetone/water 9:1, *v*/*v* **g**; spray-dried STNA in CCM from acetone/water 9:1 (*v*/*v*), heated up to 155 °C **h**; spray-dried STNA in CCM from acetone/water 9:1 (*v*/*v*), heated up to 170 °C **i**; spray-dried STNA in CCM from acetone/water 9:1 (*v*/*v*), heated up to 230 °C **j**; and spray-dried STNA in OCM from ethanol/water 9:1 (*v*/*v*), heated up to 180 °C **k**

DISCUSSION

Sulfathiazole

As clearly shown from PXRD diffraction and confirmed by thermal analysis data, powders of metastable ST polymorph I were produced by using the CCM configuration of the lab-scale spray drier using nitrogen as the drying gas, whilst amorphous powders of ST were obtained from ethanolic solutions in the OCM configuration. These results agreed with the findings of Islam and Langrish (12) who demonstrated how the selection of different spray drier configurations and drying gas could affect the properties of spray-dried lactose. Different equipment configurations and the use of different solvents will lead to different pressure, temperature and humidity environments inside the spray drier, causing variations in the heat–mass transfer which could affect the properties of the spray-dried materials. For example, it has been shown that the exposure of an amorphous system to vapours of a solvent in which the system is more soluble has a greater plasticising effect compared to a solvent in which the solubility is lower (21). The potential presence of a higher amount of ethanol vapour in the spray drier when operating in CCM compared to OCM is most likely the reason for the different outcomes obtained from changing the spray drier configuration. In theory, in the closed-loop system, the solvent contained in the gas stream is cooled and consequently condensed. The regenerated flow is then returned to the spray dryer. However, it is possible that a certain amount of the organic vapour contaminates the regenerated carrier gas. In contrast, in the open-loop system, the ethanol vapour is diluted by the environmental air (which contains water vapour) and exhausted into the atmosphere, thus affecting the crystallisation process to a lesser extent. Interestingly, only ST spray-dried from pure ethanol in the OCM was partially crystalline. The residual crystallinity in the sulfathiazole spray-dried from pure ethanol can be related to the use of an oversaturated

solution. It is possible that the initial evaporation of solvent results in the sulfathiazole precipitating from the supersaturated solution, resulting in a suspension and, subsequently, a crystalline dried solid, in contrast to solvent evaporation from an undersaturated solution which results in amorphous solids. Unexpectedly, solvent selection and feed concentration appeared not to affect the solid-state nature of ST when the API was spray-dried in the CCM. In contrast, numerous reports in the literature describe ST as a compound that can be isolated in at least five different polymorphic forms and that the solidification from solution into a specific polymorph or into mixtures of polymorphs can be determined by the choice of: solvent, type of crystallisation process and parameters used in the crystallisation process (2,20,22–24).

The differences between the results presented here and the aforementioned results of crystallisation studies can be attributed to the nature of the process employed in our study. Although based on the same principles of solvent removal and solidification of solute, spray drying and crystallisation by solvent evaporation are characterised by different kinetics. In the latter process, at supersaturation, form I starts to nucleate regardless of the solvent employed in the process, which implies that ST molecules are connected in α dimers, basic units of polymorph I (2,20). At a certain stage, the metastable form I will start to dissolve, and β-dimers, basic units of polymorphs II–V (2,16,20), if not thermodynamically inhibited, will subsequently develop, leading to a different crystalline polymorph (the next most stable). In spray drying, both the rupture of the α-dimer bonds and the formation of β-dimers are suppressed/inhibited due to the kinetics of the solvent evaporation process. Atomisation of the liquid feed and the drying step are extremely rapid, and the metastable form has to remain suspended in the solvent to favour its phase transition to the next more stable form. In our study, it was found that spray-dried powders obtained from ethanolic solutions in the OCM under air drying were amorphous and physically unstable. Solvent removal did not allow the
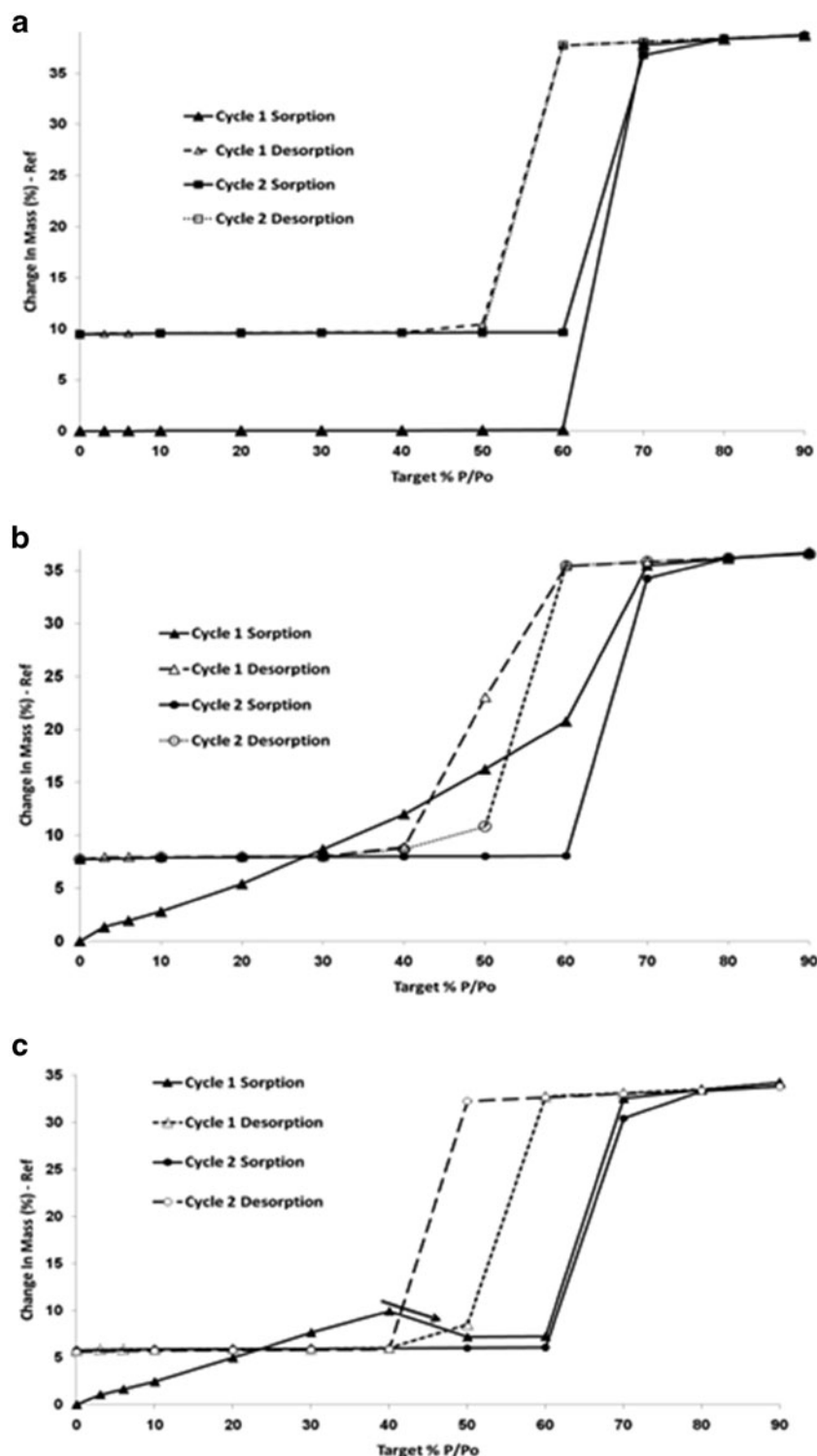
Fig. 8. DVS sorption–desorption isotherms of unprocessed STNA **a**; spray-dried STNA in OCM from ethanol/water 9:1, *v/v* **b**; and spray-dried STNA in CCM from acetone/water 9:1, *v/v* **c**

nucleation of ST form I in the OCM, leading to an amorphous material. In contrast to the work of Caron *et al.* (7), who previously obtained ST form I upon spray drying in the OCM with an inlet temperature of 85 °C, the use of an inlet temperature of 78 °C in the current study induced a reduction of the outlet temperature below the T_g of the drug (~59 °C), resulting in ST being obtained in its amorphous state. In contrast to other studies, this work investigates the amorphous ST obtained without employing the melt quench technique, a technique which is usually successful in the production of amorphous materials, but often characterised by degradation of the materials and considered not suitable for large-scale manufacturing.
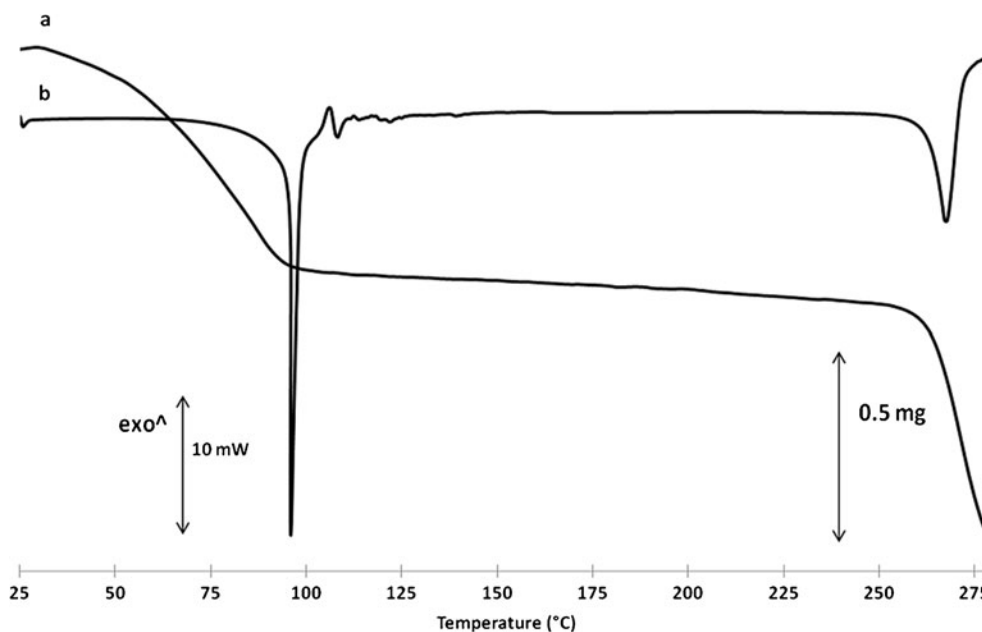
Fig. 9. DSC **a** and TGA **b** thermograms of spray-dried STNA in OCM from ethanol/water 9:1 (*v/v*) after DVS analysis

The close similarity of the Fourier transform infrared (FTIR) spectra of the amorphous form to form I compared to form III, in particular in the NH stretching peak region (data not shown) and the crystallisation behaviour of ST from the amorphous state under different storage conditions and upon heating in the DSC oven, leads us to hypothesise that the short-range molecular order of amorphous ST might be represented by α-dimers. Amorphous ST powders tend to crystallise rapidly and at even low relative humidity. An analogy between the crystallisation of ST from solution and from its amorphous state is evident. In both cases, the first form to nucleate is form I. The amorphous material was seen to partially crystallise into form I up to 1 h from the end of the spray drying process (Fig. 1) regardless of the environmental conditions, consistent with Ostwald's rule of stages. Keeping material in dry conditions below 35 % of RH led to a full transformation into pure form I, whilst keeping it at RH above 35 % led to crystallisation towards a mixture of forms I, III and/or II (the close similarity between the PXRD patterns of forms II and III (Fig. 1) does not allow the identification of which ST polymorph or mixtures of polymorphs are developing together with form I upon different storage conditions). The low-humidity conditions prevent the formation of β-dimers which necessitate ST molecules to be solvated, and it is hypothesised that the α-dimers already present in the amorphous structure are the reason why form I rapidly develops within the material under dry conditions of storage. In contrast, high RH provided the environmental conditions necessary to favour the formation of β-dimers and, consequently, the crystallisation of the amorphous material into a mixture of polymorphs.

Another important observation from the current work is that spray drying allowed spherical particles of ST form I with rough surfaces to be generated, which is in contrast to the typical morphology reported in the literature for form I following conventional crystallisation processes. According to the literature, the morphological representation of ST form I

and typical of several metastable polymorphs is needle-like (2,20,25), a morphology which is usually considered adverse for pharmaceutical development (26).

Sulfathiazole Sodium

Ensuring the physical stability of amorphous systems is essential to exploit their likely favourable properties. As a strategy to succeed in the development of a more stable amorphous form, the spray drying process was tested on the sodium salt of ST. The remarkable rise in melting point (~268 °C) with respect to the corresponding non-salt form (~201 °C) is attributed to an increased stability due to the introduction of ionic interactions within the crystalline structure (27). The sodium salt of ST converted to an amorphous phase upon processing, but in this case regardless of the solvent employed and spray drier setup. A significant increase of T_g in the amorphous salt with respect to the amorphous ST confirmed the influence of the counterion on the thermal properties of the amorphous material, as was previously reported by Tong and Zografi (27) for indomethacin sodium.

However, the spray drier setup, solvent selection and ratio affected the thermal features of the processed salt. For example, STNa spray-dried from pure ethanol and ethanol/water 9:1 (*v/v*) in the CCM crystallised at a lower temperature compared to the same systems spray-dried in the OCM. Corresponding TGA analysis showed that the two samples spray-dried in the CCM were characterised by mass loss up to 150 °C. In contrast, the same samples spray-dried in the OCM presented mass loss between 25 and 130 °C. Thus, solvent molecules appear to be more strongly retained in the amorphous samples spray-dried in CCM, causing a decrease in the onset of crystallisation. Likewise, the deflection of the baseline attributed to the T_g of the material spray-dried from acetone water 9:1 (*v/v*) in the CCM was recorded at a lower temperature compared to the systems spray-dried in the OCM. MDSC analysis showed that the glass transition deflection in the acetonic system was in two steps. A

double T_g might explain this result from MDSC analysis: the first T_g would represent the change in heat capacity for a certain proportion of amorphous material exposed to acetone, the second T_g represented by the remaining dry material. The FTIR spectra (data not shown) of amorphous STNa processed from acetone/water presented a peak at ~1,700 cm^{-1}. This peak is typical of the CO stretching vibration of ketones. It was not found in the spectra of either the original material or the processed materials from water and ethanol/water solvent systems and therefore attributed to the acetone retained in the amorphous salt. In addition, TGA analysis recorded a ~1 % mass loss from the material spray-dried from acetone/water 9:1 (v/v) in the CCM at a temperature corresponding to the crystallisation of the material from the amorphous state. This mass loss may be attributed to the release of solvent upon crystallisation, confirming the presence of solvent retained in the amorphous material.

Complementary methods (DSC and PXRD) were useful to demonstrate the ability of STNa to give rise to polymorphism when subjected to thermal stress. All amorphous samples spray-dried in the OCM and the samples spray-dried from ethanol/water in the CCM, when the water content in the solvent was 20 % (v/v) or more, crystallised into a different crystal structure compared to the starting material. This new polymorph then reconverted to the original material with a further rise in temperature. In contrast, amorphous STNa spray-dried from acetone/water in the CCM after complete crystallisation was found to be a mixture of the two polymorphic forms. Only amorphous STNa spray-dried from ethanol and ethanol/water 9:1 (v/v) in the CCM crystallised directly into the original structure at a temperature ~20 °C lower than the other systems. Solvent retained in the amorphous structure seems to play an important role in the crystallisation from the amorphous state upon heating.

Higher T_g (~120 °C) and onset of crystallisation led to an increased physical stability of the amorphous salt compared to amorphous ST in dry conditions. The recommended storage temperature for amorphous materials has to be at least 50 °C lower than the T_g in order to reduce the molecular mobility close to zero [28]. Hence, the storage temperature of 4 °C did not induce the crystallisation of the amorphous salt. Though the T_g of amorphous STNa was higher than that of amorphous ST, RH was found to have a strong plasticising effect inducing the phase transformation of the salt into a hydrate form when exposed to a full cycle (0–90–0 %) of step changes in RH. After DVS treatment, the PXRD patterns of both the processed salt samples and of unprocessed STNa were identical. These patterns differed from the pattern of the original material (*i.e.* not subjected to DVS analysis), indicating a change in the crystal structure. The shortfall in the mass gain percentage in the amorphous systems of ~1.7 and ~3.7 % for the ethanolic and acetonic systems, respectively, compared to the final mass gain percentage of the original material subjected to DVS can be attributed to the solvent retained in the amorphous form at the beginning of the experiment. This solvent does not separate from the powder during the pretreatment phase (drying at 0 % RH in the DVS apparatus until constant mass). Several hydrates of STNa are reported in the literature [29]. A mass uptake per cent of 9.5± 0.1 at the end of a full DVS cycle experiment for unprocessed

STNa is consistent with the theoretical stoichiometric water content for a sesquihydrate. Interestingly, the DVS sorption profiles were different for different spray-dried samples. No loss of mass was detected in the first sorption isotherm for STNa spray-dried from either water or ethanol/water 9:1 (v/v). Therefore, it would appear that the amorphous material converts directly to a hydrated crystal form with the increase of RH. In contrast, the amorphous salt spray-dried from acetone/water 9:1 (v/v) showed mass loss in the RH step between 40 and 50 %. Mass loss is hypothesised to be due to the loss of acetone. The acetone retained in the amorphous powder is released from the material during the crystallisation stage, indicating a higher affinity of the solvent for the amorphous structure of the drug compared to ethanol.

CONCLUSION

The solid-state characteristics of a drug can be controlled by careful adjustment of the processing and/or storage parameters. This study shows that spray drying may be used as an alternative technique to "classic" crystallisation from solvent evaporation, especially when dealing with highly polymorphic systems. Its advantage lies in producing pure metastable polymorphs with no needle-like morphology which traditionally may be hard to achieve with slow evaporation techniques. Furthermore, spray drying settings can be tuned to generate amorphous states, and we have demonstrated that properties of amorphous material can be altered by producing an amorphous salt form. The exploitation of an amorphous salt form would appear to be of potential interest if characterised by low hygroscopicity or if storage conditions are carefully controlled and may be applicable to several active pharmaceutical ingredients.

ACKNOWLEDGEMENTS

REFERENCES

1. Tajber L, Corrigan OI, Healy AM. Physicochemical evaluation of PVP-thiazide diuretic interactions in co-spray-dried composites—analysis of glass transition composition relationships. Eur J Pharm Sci. 2005;24(5):553–63.
2. Parmar MM, Khan O, Seton L, Ford JL. Polymorph selection with morphology control using solvents. Cryst Growth Des. 2007;7(9):1635–42.
3. Huang LF, Tong WQ. Impact of solid state properties on developability assessment of drug candidates. Adv Drug Deliv Rev. 2004;56(3):321–34.
4. Hancock BC, Zografi G. Characteristics and significance of the amorphous state in pharmaceutical systems. J Pharm Sci. 1997;86 (1):X1–X12.
5. Rodríguez-Spong B, Price CP, Jayasankar A, Matzger AJ, Rodríguez-Hornedo N. General principles of pharmaceutical solid polymorphism: a supramolecular perspective. Adv Drug Deliv Rev. 2004;56(3):241–74.
6. Mortko CJ, Sheth AR, Variankaval N, Li L, Farrer BT. Risk assessment and physicochemical characterization of a metastable dihydrate API phase for intravenous formulation development. J Pharm Sci. 2010;99(12):4973–81.

7. Caron V, Tajber L, Corrigan OI, Healy AM. A comparison of spray drying and milling in the production of amorphous dispersions of sulfathiazole/polyvinylpyrrolidone and sulfadimidine/polyvinylpyrrolidone. Mol Pharmaceutics 2011;8(2):532–42.

8. Master K. Spray drying in practice. SprayDryConsult International ApS Denmark. 2002.

9. Chidavaenzi OC, Buckton G, Koosha F, Pathak R. The use of thermal techniques to assess the impact of feed concentration on the amorphous content and polymorphic forms present in spray dried lactose. Int J Pharm. 1997;159(1):67–74.

10. Dontireddy R, Crean AM. A comparative study of spray-dried and freeze-dried hydrocortisone/polyvinyl pyrrolidone solid dispersions. Drug Dev Ind Pharm. 2011;37(10):1141–9.

11. Janssens S, Anné M, Rombaut P, Van den Mooter G. Spray drying from complex solvent systems broadens the applicability of Kollicoat IR as a carrier in the formulation of solid dispersions. Eur J Pharm Sci. 2009;37(3–4):241–8.

12. Islam MIU, Langrish TAG. The effect of different atomizing gases and drying media on the crystallization behavior of spray-dried powders. Drying Technol. 2010;28(9):1035–43.

13. Rodríguez-Hornedo N, Murphy D. Significance of controlling crystallization mechanisms and kinetics in pharmaceutical systems. J Pharm Sci. 1999;88(7):651–60.

14. Croker D, Hodnett BK. Mechanistic features of polymorphic transformations: the role of surfaces. Cryst Growth Des. 2010;10(6):2808–16.

15. Hu Y, Erxleben A, Ryder AG, McArdle P. Quantitative analysis of sulfathiazole polymorphs in ternary mixtures by attenuated total reflectance infrared, near-infrared and Raman spectroscopy. J Pharm Biomed Anal. 2010;53(3):412–20.

16. Chan FC, Anwar J, Cernik R, Barnes P, Wilson RM. Ab initio structure determination of sulfathiazole polymorph V from synchrotron X-ray powder diffraction data. J Appl Crystallogr. 1999;32(3):436–41.

17. Capparella M, Foster III W, Larrousse M, Phillips DJ, Pomfret A, Tuvim Y. Characteristics and applications of a new high-performance liquid chromatography guard column. J Chromatogr A. 1995;691(1–2):141–50.

18. Tewes F, Tajber L, Corrigan OI, Ehrhardt C, Healy AM. Development and characterisation of soluble polymeric particles for pulmonary peptide delivery. Eur J Pharm Sci. 2010;41(2):337–52.

19. Zeitler JA, Newnham DA, Taday PF, Threlfall TL, Lancaster RW, Berg RW, *et al.* Characterization of temperature-induced phase transitions in five polymorphic forms of sulfathiazole by terahertz pulsed spectroscopy and differential scanning calorimetry. J Pharm Sci. 2006;95(11):2486–98.

20. Blagden N, Davey RJ, Lieberman HF, Williams L, Payne R, Roberts R, *et al.* Crystal chemistry and solvent effects in polymorphic systems: sulfathiazole. J Chem Soc—Faraday Trans. 1998;94(8):1035–44.

21. Yoshioka A, Tashiro K. Solvent effect on the glass transition temperature of syndiotactic polystyrene viewed from time-resolved measurements of infrared spectra at the various temperatures and its simulation by molecular dynamics calculation. Macromolecules. 2004;37(2):467–72.

22. Aaltonen J, Rantanen J, Siiriä S, Karjalainen M, Jørgensen A, Laitinen N, *et al.* Polymorph screening using near-infrared spectroscopy. Anal Chem. 2003;75(19):5267–73.

23. Khoshkhoo S, Anwar J. Crystallization of polymorphs: the effect of solvent. J Phys D: Appl Phys. 1993;26(8B):B90.

24. Anwar J, Tarling SE, Barnes P. Polymorphism of sulfathiazole. J Pharm Sci. 1989;78(4):337–42.

25. McArdle P, Hu Y, Lyons A, Dark R. Predicting and understanding crystal morphology: the morphology of benzoic acid and the polymorphs of sulfathiazole. Cryst Eng Comm. 2010;12(10):3119–25.

26. Cuppen HM, Van Eerd ART, Meekes H. Needlelike morphology of aspartame. Cryst Growth Des. 2004;4(5):989–97.

27. Tong P, Zografi G. Solid-state characteristics of amorphous sodium indomethacin relative to its free acid. Pharm Res. 1999;16(8):1186–92.

28. Hancock BC, Shamblin SL, Zografi G. Molecular mobility of amorphous pharmaceutical solids below their glass transition temperatures. Pharm Res. 1995;12(6):799–806.

29. Rubino JT. Solubilities and solid state properties of the sodium salts of drugs. J Pharm Sci. 1989;78(6):485–9.